

1-1-2013

Flux pinning mechanism in BaFe_{1.9}Ni_{0.1}As₂ single crystals: Evidence for fluctuation in mean free path induced pinning

M Shahbazi-Manshadi

University of Wollongong, msm979@uowmail.edu.au

X L Wang

University of Wollongong, xiaolin@uow.edu.au

K Y Choi

Sogang University, Tohoku University, Seoul National University

S X. Dou

University of Wollongong, shi@uow.edu.au

Follow this and additional works at: <https://ro.uow.edu.au/aiimpapers>



Part of the [Engineering Commons](#), and the [Physical Sciences and Mathematics Commons](#)

Recommended Citation

Shahbazi-Manshadi, M; Wang, X L; Choi, K Y; and Dou, S X., "Flux pinning mechanism in BaFe_{1.9}Ni_{0.1}As₂ single crystals: Evidence for fluctuation in mean free path induced pinning" (2013). *Australian Institute for Innovative Materials - Papers*. 814.

<https://ro.uow.edu.au/aiimpapers/814>

Flux pinning mechanism in BaFe_{1.9}Ni_{0.1}As₂ single crystals: Evidence for fluctuation in mean free path induced pinning

Abstract

The flux pinning mechanism of BaFe_{1.9}Ni_{0.1}As₂ superconducting crystals have been investigated systematically by magnetic measurements up to 13 T at various temperatures. The field dependence of the critical current density, J_c , was analysed within the collective pinning model. A remarkably good agreement between the experimental results and theoretical J_c pinning curve is obtained, which indicates that pinning in BaFe_{1.9}Ni_{0.1}As₂ crystal originates from spatial variation of the mean free path. Moreover, the normalized pinning force density, F_p , curves versus $h/4B/B_{irr}$ (B_{irr} is the irreversibility field) were scaled using the Dew-Hughes model. Analysis suggests that point pinning alone cannot explain the observed field variation of F_p .

Keywords

pinning, mechanism, bafe1, 9ni0, 1as2, flux, single, mean, crystals, evidence, fluctuation, induced, path, free

Disciplines

Engineering | Physical Sciences and Mathematics

Publication Details

Shahbazi-Manshadi, M., Wang, X., Choi, K. & Dou, S. X. (2013). Flux pinning mechanism in BaFe_{1.9}Ni_{0.1}As₂ single crystals: Evidence for fluctuation in mean free path induced pinning. *Applied Physics Letters*, 103 (3), 032605-1-032605-4.

Flux pinning mechanism in BaFe_{1.9}Ni_{0.1}As₂ single crystals: Evidence for fluctuation in mean free path induced pinning

M. Shahbazi, X. L. Wang, K. Y. Choi, and S. X. Dou

Citation: *Appl. Phys. Lett.* **103**, 032605 (2013); doi: 10.1063/1.4813113

View online: <http://dx.doi.org/10.1063/1.4813113>

View Table of Contents: <http://apl.aip.org/resource/1/APPLAB/v103/i3>

Published by the AIP Publishing LLC.

Additional information on Appl. Phys. Lett.

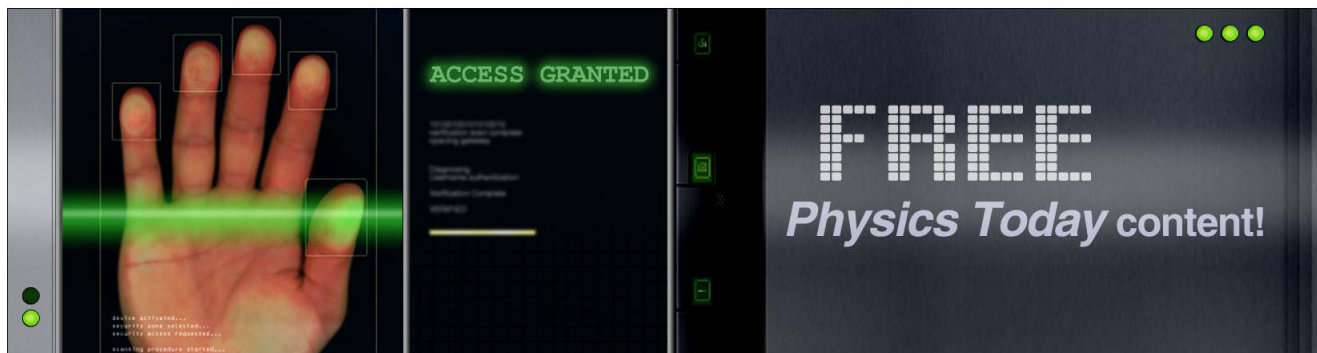
Journal Homepage: <http://apl.aip.org/>

Journal Information: http://apl.aip.org/about/about_the_journal

Top downloads: http://apl.aip.org/features/most_downloaded

Information for Authors: <http://apl.aip.org/authors>

ADVERTISEMENT



Flux pinning mechanism in $\text{BaFe}_{1.9}\text{Ni}_{0.1}\text{As}_2$ single crystals: Evidence for fluctuation in mean free path induced pinning

M. Shahbazi,¹ X. L. Wang,^{1,a)} K. Y. Choi,² and S. X. Dou¹

¹*Institute for Superconducting and Electronic Materials, University of Wollongong, North Wollongong, NSW 2519, Australia*

²*Center for Novel States of Complex Materials Research, Department of Physics and Astronomy, Seoul National University, Seoul 151-747, South Korea*

(Received 10 April 2013; accepted 17 June 2013; published online 19 July 2013)

The flux pinning mechanism of $\text{BaFe}_{1.9}\text{Ni}_{0.1}\text{As}_2$ superconducting crystals have been investigated systematically by magnetic measurements up to 13 T at various temperatures. The field dependence of the critical current density, J_c , was analysed within the collective pinning model. A remarkably good agreement between the experimental results and theoretical δl pinning curve is obtained, which indicates that pinning in $\text{BaFe}_{1.9}\text{Ni}_{0.1}\text{As}_2$ crystal originates from spatial variation of the mean free path. Moreover, the normalized pinning force density, F_p , curves versus $h = B/B_{irr}$ (B_{irr} is the irreversibility field) were scaled using the Dew-Hughes model. Analysis suggests that point pinning alone cannot explain the observed field variation of F_p . © 2013 AIP Publishing LLC. [<http://dx.doi.org/10.1063/1.4813113>]

Study of the vortex mechanisms in pnictides is crucial for practical applications due to relatively high critical temperature, T_c , high upper critical field, B_{c2} , high J_c , very high intrinsic pinning potential,² and nearly isotropic superconductivity^{3,4} of these compounds. The 122 family, AFe_2As_2 has attracted great interest for the study of superconducting properties due to their simple crystal structures and possibility of growing large single crystals.^{5,6}

For some superconductors, the J_c obtained from magnetic hysteresis loops (MHLs), increases with magnetic field after the first peak of penetration field. This is the so-called second magnetization peak (SMP) or fishtail effect. In conventional low temperature superconductors, e.g., MgB_2 ,⁷ Nb_3Sn ,⁸ etc., SMP corresponds to a hump feature in $J_c(B)$ far below the B_{c2} while peak effect (PE) is realized to happen near B_{c2} .⁹ It is suggested that the PE is associated with the rapid softening of the flux line lattice.¹⁰ In high temperature superconductors, different mechanisms including inhomogeneity of the sample,¹¹ Dynamic effects,¹² structural phase transition in the vortex lattice,¹³ vortex order-disorder phase transition,^{14,15} and cross over from elastic to plastic creep¹⁶ have been proposed to explain the SMP. It is reported SMP occur in $\text{SmFeAsO}_{0.9}\text{F}_{0.1}$ (Ref. 17) as a result of weak and collective pinning of the system. The SMP observed only for the samples near optimally doping for $\text{NdFeAsO}_{0.85}$,¹⁸ $\text{Ba}(\text{Fe}_{1-x}\text{Co}_x)_2\text{As}_2$ (Refs. 19–22) and weak and collective pinning are concluded for most studies. The SMP has also been observed in optimally doped $\text{Ba}_{1-x}\text{K}_x\text{Fe}_2\text{As}_2$.^{19,23} However, it is worth to note that most form of in-homogeneity like T_c variation, impurity phase, doping variation, etc., might prevent the occurrence of SMP.²⁴ For example, an under-doped $\text{Ba}_{1-x}\text{K}_x\text{Fe}_2\text{As}_2$ system does not show the SMP. Also SMP has been reported for $\text{Ba}(\text{Fe}_{1-x}\text{Ni}_x)_2\text{As}_2$,^{19,25} LiFeAs ,²⁶ $\text{FeTe}_{1-x}\text{Se}_x$ (Ref. 27), and $\text{PrFeAsO}_{0.6}\text{F}_{0.1}$.²⁸ The observed SMP for electron and hole doped Ba-122 crystals for $H//c$ ¹⁹ was disappeared for $H//ab$,

indicating an anisotropic effect of flux pinning for these compounds.¹⁹

There are two main pinning mechanisms in type II superconductors: (I) δl pinning from spatial variation in the charge carrier mean free path, l , and (II) δT_c pinning due to randomly distributed spatial variation in T_c . It has been reported that strong pinning centres in $\text{PrFeAsO}_{0.9}$ and $\text{NdFeAsO}_{0.9}\text{F}_{0.1}$ arise from oxygen deficiency and dopant atoms, which results in pinning by local variations in the mean-free path.²⁹ Strong intrinsic pinning due to structural domains in the superconducting orthorhombic phase³⁰ of $\text{Ba}(\text{Fe}_{1-x}\text{Co}_x)_2\text{As}_2$ is also observed. Similar results were found for $\text{BaFe}_{1.8}\text{Co}_{0.2}\text{As}_2$, where the temperature and field dependence of J_c were attributed to the inhomogeneous distribution of Co atoms.³¹ Furthermore, *It has been suggested* that the very large J_c and fishtail effect at high temperature below T_c in $\text{Ba}_{0.6}\text{K}_{0.4}\text{Fe}_2\text{As}_2$ had originated from the small-size normal core pinning centres.²³

In this work, we present a systematic study of the flux pinning mechanism of $\text{BaFe}_{1.9}\text{Ni}_{0.1}\text{As}_2$ crystals.

Single crystal of $\text{BaFe}_{1.9}\text{Ni}_{0.1}\text{As}_2$ was prepared by a self-flux method.^{32,33} For magnetic measurements, the as-grown single crystal was cleaved and cut into a rectangular shape. The present $\text{BaFe}_{1.9}\text{Ni}_{0.1}\text{As}_2$ sample has dimensions of $1.56 \times 2.82 \times 0.06 \text{ mm}^3$. Magnetization loops were collected in different magnetic fields with $B//c$ and at temperatures down to 3 K using a superconducting quantum interference device vibrating sample magnetometer (SQUID-VSM, Quantum Design).

The inset of Fig. 1 shows the temperature dependence of the magnetization measured after zero-field-cooling (ZFC) and field-cooling (FC) of the $\text{BaFe}_{1.9}\text{Ni}_{0.1}\text{As}_2$ crystal, with a field of 200 Oe for $B//c$. The T_c of 17.7 K was determined from the onset of the transition. The MHLs of the $\text{BaFe}_{1.9}\text{Ni}_{0.1}\text{As}_2$ crystal at $3 \text{ K} < T < 15 \text{ K}$ for $B//c$, are shown in the main panel of Fig. 1. The almost perfect symmetry of the MHLs with respect to the x-axis indicates that bulk pinning is dominant.²⁵ The minimum in the magnetization, which is located slightly above

^{a)} Author to whom correspondence should be addressed. Electronic mail: xiaolin@uow.edu.au

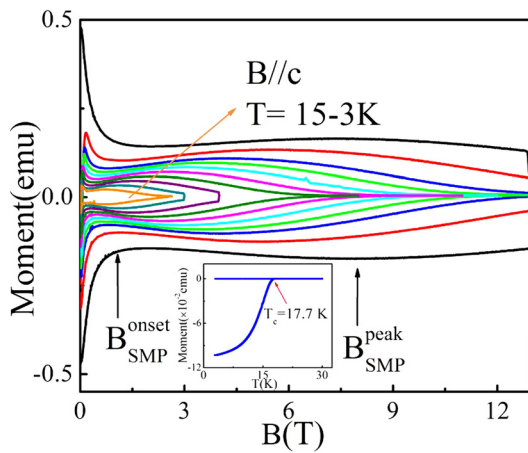


FIG. 1. MHLs at various temperatures for $B//c$. Inset: Temperature dependence of the magnetic susceptibility.

zero field in a given MHLs, characterizes the onset of SMP. At this field, the applied magnetic field penetrates completely into the bulk sample after ZFC.³⁴ The SMP can be observed at all temperatures below 15 K, similar to the behaviour of $(\text{Ba,K})\text{Fe}_2\text{As}_2$ (Ref. 23) and $\text{BaFe}_{1-x}\text{Co}_x\text{As}_2$ crystals.³¹ Arrows indicate the onset ($B_{\text{SMP}}^{\text{onset}}$) and peak ($B_{\text{SMP}}^{\text{peak}}$) positions of the SMP in Fig. 1 for $T = 3$ K. In some of the conventional superconductors, such as MgB_2 (Ref. 7) and Nb_3Sn ,⁸ the PE occurs at a field close to the B_{c2} . It is believed that the PE is associated with the metastability of an underlying first-order vortex melting transition, where softening of the vortex due to the thermal fluctuation leads to a better accommodation of the pinning centres by the vortex lattice.⁸ This explanation of the PE in Nb_3Sn does not appear to be applicable to the PE observed in cuprates and pnictides, in which PE occurs far from the normal phase boundary. In the case of cuprates, it has been suggested that a first-order disorder driven transition is responsible for SMP.³⁵ Salem-Sugui, Jr. *et al.*³⁶ studied the vortex dynamics of an over-doped $\text{BaFe}_{1.82}\text{Ni}_{0.18}\text{As}_2$ crystal by measuring flux creep over the SMP and suggested that the SMP could not arise due to the softening in the vortex pinning prior to melting nor from a change in the pinning regime within a collective model. Also, their study of an optimally doped $\text{BaFe}_{1.9}\text{Ni}_{0.1}\text{As}_2$ crystal did not show any evidence of a pinning crossover occurring near the SMP of the MHLs.²⁵ Magnetic studies by Prozorov *et al.*²¹ and Shen *et al.*²⁰ interpreted the SMP as signifying a crossover from elastic to plastic vortex creep. The same result was obtained by Kopeliansky *et al.*, who suggested that the SMP is associated with a vortex structural phase transition from a rhombic to a square lattice.²²

The J_c values were extracted from the MHLs, using Bean's model,³⁷ where $J_c(B) = 20 \times \Delta M(B) / (l(1 - l/3w))$, with l and w being the sample dimensions perpendicular to the applied magnetic field, $l < w$, and ΔM is the width of the hysteresis loops.

Figure 2 shows the field dependence of J_c at different temperatures for $B//c$. The obtained value of $J_c = 0.14 \times 10^6$ A/cm² at zero field and $T = 10$ K is comparable with the reported value of $J_c = 0.23 \times 10^6$ for the optimally doped sample.¹⁹ The inset of Figure 2 illustrates a normalized J_c versus B plot at selected temperatures. The onset position, $B_{\text{SMP}}^{\text{onset}}$, and peak position, $B_{\text{SMP}}^{\text{peak}}$, of the SMP are marked for

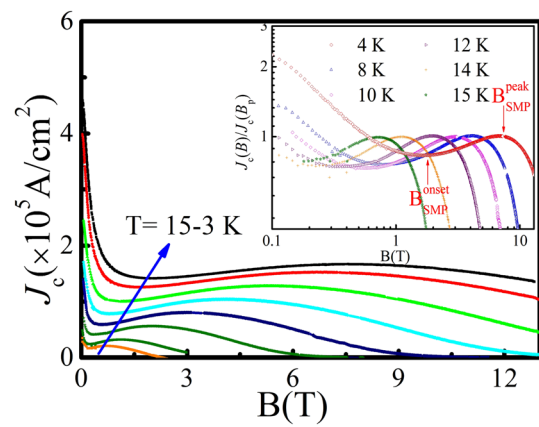


FIG. 2. Field dependence of J_c at different temperatures for $B//c$. Inset: Field dependence of the normalized J_c at different temperatures for $B//c$.

$T = 4$ K. The position of SMP shifts toward lower field with increasing temperature, for example, $B_{\text{SMP}}^{\text{peak}}$ decreases considerably from 6.8 T at 4 K to 0.7 T at 15 K, but $B_{\text{SMP}}^{\text{onset}}$ drops slowly from 1.7 T at 4 K to 0.2 T at 15 K, respectively. Similar behaviour was observed for $\text{REBa}_2\text{Cu}_3\text{O}_{7-\delta}$.³⁸ It is likely that the SMP has the same mechanism in both compounds.²³

In Fig. 3, we present the vortex phase diagram of the $\text{BaFe}_{1.9}\text{Ni}_{0.1}\text{As}_2$ crystal. Three characteristic fields, B_{irr} , $B_{\text{SMP}}^{\text{peak}}$, and $B_{\text{SMP}}^{\text{onset}}$, were determined from magnetic measurements as shown by the solid symbols in Fig. 3. It is clear that the $B_{\text{irr}} - T$, $B_{\text{SMP}}^{\text{peak}} - T$, and $B_{\text{SMP}}^{\text{onset}} - T$ are temperature dependent. The large area between $B_{\text{irr}} - T$ and $B_{\text{SMP}}^{\text{peak}} - T$ suggests that the vortex dissipation is through plastic motion in this area, as proposed by Shen *et al.* for optimally Co doped BaFe_2As_2 .²⁰ The dashed lines represent the fitting curves using $B(T) = A(1 - T/T_c)^n$, with n being a fitting parameter. All the curves were well fitted using the expression with $n = 1.9$ for $B_{\text{SMP}}^{\text{onset}}$ and $n = 1.4$ for $B_{\text{SMP}}^{\text{peak}}$ and B_{irr} . These values are similar to the values obtained for $\text{BaFe}_{2-x}\text{Co}_x\text{As}_2$ crystal.²⁰

In order to assess the nature of the pinning mechanisms in more detail, it is useful to look at the variation of the vortex pinning force, $F_p = B \times J_c$, with the magnetic field. In Fig. 4, we plot the normalized pinning force, $F_p^{\text{norm}} = F_p / F_p^{\text{max}}$, as a function of the reduced field, $h = B / B_{\text{irr}}$,

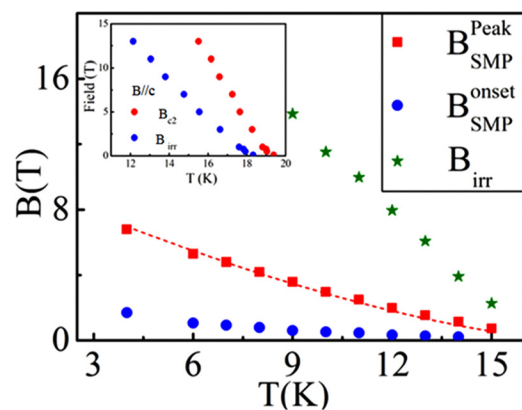


FIG. 3. Vortex phase diagram of $\text{BaFe}_{1.9}\text{Ni}_{0.1}\text{As}_2$ single crystal determined from magnetic measurements for $B//c$. Inset: Temperature dependence of B_{c2} and B_{irr} obtained from $\rho - T$ curves for $B//c$.

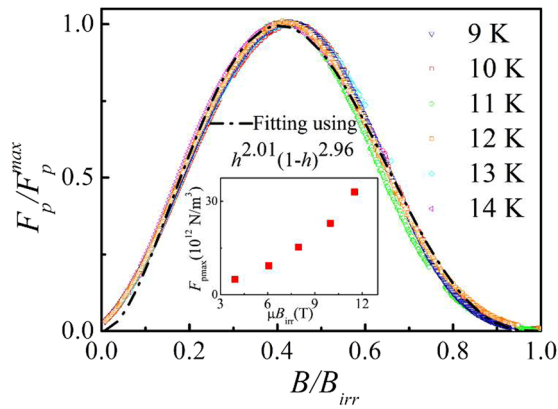


FIG. 4. Normalized flux pinning force $F_p^{norm} = F_p/F_p^{max}$ as a function of reduced field, $h = B/B_{irr}$. The dashed-dotted line represents the fitting curve $h^{2.01}(1-h)^{2.96}$. Inset: Field dependence of the maximum pinning force.

The B_{irr} is estimated using the criterion of $J_c < 100 \text{ A/cm}^2$. It should be noted the scaling of the normalized pinning force is done based on the reduced field by B_{irr} with $h = B/B_{irr}$ instead of B_{c2} with $h = B/B_{c2}$ due to the facts that the difference between B_{c2} and B_{irr} is sizable, and is more significant at low temperature regime in the case of pnictides, MgB_2 and cuprates.^{7,29,32,38,39} The temperature dependence of B_{c2} and B_{irr} obtained from ρ - T curves (see the inset in Fig. 3) clearly reveal the B_{irr} is far below the B_{c2} . Note that all the F_p^{norm} curves for $9 \text{ K} \leq T \leq 14 \text{ K}$ collapse into one unified curve. We fit these data using the Dew-Hughes formula, $F_p \propto h^p(1-h)^q$,⁴⁰ where p and q are two parameters whose values depend on the origin of the pinning mechanism. The Dew-Hughes fit is shown by the black dashed-dotted line in Fig. 4 with $p = 2.01$ and $q = 2.96$. The value $p/(p+q) \approx 0.4$ matches well with the peak positions in the F_p^{norm} versus h plots. According to the Dew-Hughes model, in the case of δl pinning for a system dominated just by point pinning, $p = 1$ and $q = 2$, with F_p^{norm} occurring at $h_{max} = 0.33$. Pinning due to grain boundaries leads to $h_{max} \approx 0.2$, while in a system in which variation in the superconducting order parameter controls the pinning mechanism, $h_{max} \approx 0.7$.^{40,41} In the case of δT_c pinning, the maximum of F_p is expected to be located at higher h values. For example, for point pinning, the maximum is expected at $h = 0.67$ with $p = 2$ and $q = 1$. For surface pins, the maximum exists at $h = 0.6$, $p = 1.5$, and $q = 1$, and for volume pins, $h = 0.5$ with $p = 1$ and $q = 1$. In our case, $h_{max} = 0.4$, indicating that point pinning alone cannot explain the pinning mechanism in the $\text{BaFe}_{1.9}\text{Ni}_{0.1}\text{As}_2$ crystal. Similar analysis has been done for $\text{Ba}_{0.68}\text{K}_{0.32}\text{Fe}_2\text{As}_2$ ($h_{max} = 0.43$), $\text{BaFe}_{1.85}\text{Co}_{0.15}\text{As}_2$ ($h_{max} = 0.37$), and $\text{BaFe}_{1.91}\text{Ni}_{0.09}\text{As}_2$ ($h_{max} = 0.33$) by Sun *et al.*¹⁹ They noticed that B_{c2} and B_{SMP}^{peak} decrease faster with decreasing temperature for $\text{BaFe}_{1.91}\text{Ni}_{0.09}\text{As}_2$ compared to $\text{Ba}_{0.68}\text{K}_{0.32}\text{Fe}_2\text{As}_2$ and $\text{BaFe}_{1.85}\text{Co}_{0.15}\text{As}_2$ crystals, which is related to the inhomogeneity in $\text{BaFe}_{1.91}\text{Ni}_{0.09}\text{As}_2$. The fact that the strongest pinning is in $\text{Ba}_{0.68}\text{K}_{0.32}\text{Fe}_2\text{As}_2$ among these three systems indicates that inhomogeneous distribution of dopants or As deficiency cannot play a crucial role in determining strong pinning in pnictides. Yang *et al.* proposed that the obtained value of $h_{max} = 0.33$ should be attributed to the small-size normal cores, as in the case of arsenic deficiency in $(\text{Ba,K})\text{Fe}_2\text{As}_2$ crystal.²³ In the case of $\text{BaFe}_{1.8}\text{Co}_{0.2}\text{As}_2$, a peak at

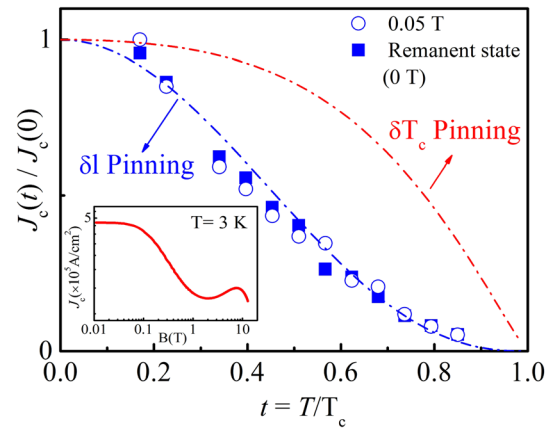


FIG. 5. Temperature dependence of the normalized measured J_c at 0.05 T (open circle) and 0 T (solid square). Inset: Field dependence of J_c at $T = 3 \text{ K}$.

$h_{max} \approx 0.45$ was suggested to be related to the inhomogeneous distribution of Co ions.³¹ In particular, the fact that, in our case, the maximum in F_p occurs at $h < 0.5$ indicates that the pinning centres in $\text{BaFe}_{1.9}\text{Ni}_{0.1}\text{As}_2$ are of the δl type, while for δT_c pinning, it is expected that the maximum would occur at $h > 0.5$.

With the aim of understanding more about the origins of the pinning in $\text{BaFe}_{1.9}\text{Ni}_{0.1}\text{As}_2$ crystal, the experimental results were analysed using collective pinning theory. According to the theoretical approach proposed by Griessen *et al.*,⁴² in the case of δl pinning, $J_c(t)/J_c(0) \propto (1-t^2)^{5/2}(1+t^2)^{-1/2}$, while for δT_c pinning, $J_c(t)/J_c(0) \propto (1-t^2)^{7/6}(1+t^2)^{5/6}$, where $t = T/T_c$. It should be noted that the flux pinning is two dimensional in such thin film, as the correlation length along the flux lines exceeds the film thickness.⁴³ Figure 5 shows a comparison between the experimental J_c values and the theoretically expected variation within the δl and δT_c pinning mechanisms at 0.05 T (open circle) and 0 T (the so called remanent state shown by solid square). The $J_c(t)$ values have been obtained from the $J_c(B)$ curves at several temperatures. A remarkably good agreement between the experimental results and theoretical δl pinning curve is obtained. It is likely that pinning in $\text{BaFe}_{1.9}\text{Ni}_{0.1}\text{As}_2$ crystal originates from spatial variation of the mean free path. Our observation of the dominant δl pinning is in good agreement with the reported δl pinning mechanism for $\text{K}_x\text{Fe}_{2-y}\text{Se}_2$, $\text{FeSe}_{0.5}\text{Te}_{0.5}$ and $\text{FeTe}_{0.7}\text{Se}_{0.3}$ crystals at low magnetic field.

In summary, we have observed the SMP effect in $\text{BaFe}_{1.9}\text{Ni}_{0.1}\text{As}_2$ crystal. The onset and peak positions of the SMP move to lower magnetic field as the temperature is raised. Analysis using the Dew-Hughes model suggests that point pins alone cannot explain the observed field variation of the pinning force density. The maximum in F_p at $h < 0.5$ indicates that the pinning centres in $\text{BaFe}_{1.9}\text{Ni}_{0.1}\text{As}_2$ are of the δl type, while for δT_c pinning, it is expected that the maximum would occur at $h > 0.5$. In addition, a good agreement between experimental and theoretical fitting using δl pinning is obtained based on collective flux pinning model.

This work was supported by the Australian Research Council through Discovery Projects, DP1094073 and DP0770205. M. Shahbazi would like to thank Professor Jin Zou at University of Queensland for his support. K.Y. Choi

was supported by the Basic Science Research Program (Grant No. 2012-008233) and Creative Research Initiative (Grant No. 2010-0018300) funded by the Korean Federation of Science and Technology Societies.

- ¹F. Hunte, J. Jaroszynski, A. Gurevich, D. C. Larbalestier, R. Jin, A. S. Sefat, M. A. McGuire, B. C. Sales, D. K. Christen, and D. Mandrus, *Nature* **453**, 903–905 (2008).
- ²X.-L. Wang, S. R. Ghorbani, S.-I. Lee, S. X. Dou, C. T. Lin, T. H. Johansen, K. H. Müller, Z. X. Cheng, G. Peleckis, M. Shahbazi *et al.*, *Phys. Rev. B* **82**, 024525 (2010).
- ³H. Q. Yuan, J. Singleton, F. F. Balakirev, S. A. Baily, G. F. Chen, J. L. Luo, and N. L. Wang, *Nature* **457**, 565–568 (2009).
- ⁴M. Shahbazi, X. L. Wang, S. R. Ghorbani, S. X. Dou, and K. Y. Choi, *Appl. Phys. Lett.* **100**, 102601 (2012).
- ⁵C. Yanchao, L. Xingye, W. Meng, L. Huiqian, and L. Shiliang, *Supercond. Sci. Technol.* **24**, 065004 (2011).
- ⁶N. Ni, S. L. Bud'ko, A. Kreyssig, S. Nandi, G. E. Rustan, A. I. Goldman, S. Gupta, J. D. Corbett, A. Kracher, and P. C. Canfield, *Phys. Rev. B* **78**, 014507 (2008).
- ⁷M. Pissas, S. Lee, A. Yamamoto, and S. Tajima, *Phys. Rev. Lett.* **89**, 097002 (2002).
- ⁸R. Lortz, N. Musolino, Y. Wang, A. Junod, and N. Toyota, *Phys. Rev. B* **75**, 094503 (2007).
- ⁹S. Sarkar, D. Pal, P. Paulose, S. Ramakrishnan, A. Grover, C. Tomy, D. Dasgupta, B. Sarma, G. Balakrishnan, and D. Paul, *Phys. Rev. B* **64**, 144510 (2001).
- ¹⁰S. Bhattacharya and M. Higgins, *Phys. Rev. B* **49**, 10005–10008 (1994).
- ¹¹M. Daeumling, J. M. Seuntjens, and D. Larbalestier, *Nature* **346**, 332 (1990).
- ¹²L. Krusin-Elbaum, L. Civale, V. Vinokur, and F. Holtzberg, *Phys. Rev. Lett.* **69**, 2280–2283 (1992).
- ¹³R. Baruch and K. Anton, *Phys. Rev. Lett.* **83**, 844 (1999).
- ¹⁴D. Giller, A. Shaulov, R. Prozorov, Y. Abulafia, Y. Wolfus, L. Burlachkov, and Y. Yeshurun, *Phys. Rev. Lett.* **79**, 2542 (1997).
- ¹⁵B. Khaykovich, E. Zeldov, D. Majer, T. W. Li, P. H. Kes, and M. Konczykowski, *Phys. Rev. Lett.* **76**, 2555 (1996).
- ¹⁶Y. Abulafia, A. Shaulov, Y. Wolfus, R. Prozorov, L. Burlachkov, and V. Yeshurun, *Phys. Rev. Lett.* **77**, 1596 (1996).
- ¹⁷H. Yang, C. Ren, L. Shan, and H.-H. Wen, *Phys. Rev. B* **78**, 092504 (2008).
- ¹⁸J. D. Moore, L. F. Cohen, Y. Yeshurun, A. D. Caplin, K. Morrison, K. A. Yates, C. M. McGilvery, J. M. Perkins, D. W. McComb, C. Trautmann *et al.*, *Supercond. Sci. Technol.* **22**, 125023 (2009).
- ¹⁹D. L. Sun, Y. Liu, and C. T. Lin, *Phys. Rev. B* **80**, 144515 (2009).
- ²⁰B. Shen, P. Cheng, Z. Wang, L. Fang, C. Ren, L. Shan, and H.-H. Wen, *Phys. Rev. B* **81**, 014503 (2010).
- ²¹R. Prozorov, N. Ni, M. A. Tanatar, V. G. Kogan, R. T. Gordon, C. Martin, E. C. Blomberg, P. Proumapan, J. Q. Yan, S. L. Bud'ko *et al.*, *Phys. Rev. B* **78**, 224506 (2008).
- ²²R. Kopeliansky, A. Shaulov, B. Y. Shapiro, Y. Yeshurun, B. Rosenstein, J. J. Tu, L. J. Li, G. H. Cao, and Z. A. Xu, *Phys. Rev. B* **81**, 092504 (2010).
- ²³H. Yang, H. Luo, Z. Wang, and H.-H. Wen, *Appl. Phys. Lett.* **93**, 142506 (2008).
- ²⁴J. T. Park, D. S. Inosov, C. Niedermayer, G. L. Sun, D. Haug, N. B. Christensen, R. Dinnebier, A. V. Boris, A. J. Drew, L. Schulz *et al.*, *Phys. Rev. Lett.* **102**, 117006 (2009).
- ²⁵S. Salem-Sugui, Jr., L. Ghivelder, A. D. Alvarenga, L. F. Cohen, H. Luo, and X. Lu, e-print [arXiv:1209.1594v1](https://arxiv.org/abs/1209.1594v1).
- ²⁶A. K. Pramanik, L. Harnagea, C. Nacke, A. U. B. Wolter, S. Wurmehl, V. Kataev, and B. Büchner, *Phys. Rev. B* **83**, 094502 (2011).
- ²⁷M. Bonura, E. Giannini, R. Viennois, and C. Senatore, *Phys. Rev. B* **85**, 134532 (2012).
- ²⁸D. Bhoi, P. Mandal, P. Choudhury, S. Dash, and A. Banerjee, *Physica C* **471**, 258–264 (2011).
- ²⁹C. J. van der Beek, G. Rizza, M. Konczykowski, P. Fertey, I. Monnet, T. Klein, R. Okazaki, M. Ishikado, H. Kito, A. Iyo *et al.*, *Phys. Rev. B* **81**, 174517 (2010).
- ³⁰R. Prozorov, M. A. Tanatar, N. Ni, A. Kreyssig, S. Nandi, S. L. Bud'ko, A. I. Goldman, and P. C. Canfield, *Phys. Rev. B* **80**, 174517 (2009).
- ³¹A. Yamamoto, J. Jaroszynski, C. Tarantini, L. Balicas, J. Jiang, A. Gurevich, D. C. Larbalestier, R. Jin, S. Sefat, M. A. McGuire *et al.*, *Appl. Phys. Lett.* **94**, 062511 (2009).
- ³²Y. Liu, R. K. Kremer, and C. T. Lin, *EPL* **92**, 57004 (2010).
- ³³Y. Liu and C. T. Lin, *J. Supercond. Novel Magn.* **24**, 183–187 (2011).
- ³⁴P. Das, A. D. Thakur, A. K. Yadav, C. V. Tomy, M. R. Lees, G. Balakrishnan, S. Ramakrishnan, and A. K. Grover, *Phys. Rev. B* **84**, 214526 (2011).
- ³⁵N. Avraham, B. Khaykovich, Y. Myasoedov, M. Rappaport, H. Shtrikman, D. E. Feldman, T. Tamegai, P. H. Kes, M. Li, M. Konczykowski *et al.*, *Nature* **411**, 451–454 (2001).
- ³⁶S. Salem-Sugui, Jr., L. Ghivelder, A. D. Alvarenga, L. F. Cohen, H. Luo, and X. Lu, *Phys. Rev. B* **84**, 052510 (2011).
- ³⁷C. P. Bean, *Phys. Rev. Lett.* **8**, 250–253 (1962).
- ³⁸U. Welp, W. K. Kwok, G. W. Crabtree, K. G. Vandervoort, and J. Z. Liu, *Appl. Phys. Lett.* **57**, 84 (1990).
- ³⁹T. Matsushita, J. Tanigawa, M. Kiuchi, A. Yamamoto, J.-i. Shimoyama, and K. Kishio, *Jpn. J. Appl. Phys., Part 1* **51**, 123103 (2012).
- ⁴⁰D. Dew-Hughes, *Philos. Mag.* **30**, 293–305 (1974).
- ⁴¹A. M. Campbell, J. E. Evetts, and D. Dewhughes, *Philos. Mag.* **18**, 313 (1968).
- ⁴²R. Griessen, H.-h. Wen, A. J. J. van Dalen, B. Dam, J. Rector, H. G. Schnack, S. Libbrecht, E. Osquiguil, and Y. Bruynseraede, *Phys. Rev. Lett.* **72**, 1910–1913 (1994).
- ⁴³K. Kimura, M. Kiuchi, E. S. Otabe, T. Matsushita, S. Miyata, A. Ibi, Y. Yamada, and Y. Shiohara, *Physica C* **463–465**, 697–701 (2007).